LLM-TPF: Multiscale Temporal Periodicity-Semantic Fusion LLMs for Time Series Forecasting

Qihong Pan[1,2] , Haofei Tan[1,2] , Guojiang Shen[1,2] , Xiangjie Kong[1,2]* , Mengmeng Wang[1,2] and Chenyang Xu[1,2]

[1]College of Computer Science and Technology, Zhejiang University of Technology, Zhejiang, China
[2]Zhejiang Key Laboratory of Visual Information Intelligent Processing, Zhejiang, China
{qihongpan, gjshen1975}@zjut.edu.cn, {haofei_tan,chen.yang.xu}@outlook.com, xjkong@ieee.org, mengmengwang@zju.edu.cn

Abstract

Large language models have demonstrated remarkable generalization capabilities and strong performance across various fields. Recent research has highlighted their significant potential in time series forecasting. However, time series data often exhibit complex periodic characteristics, posing a substantial challenge in enabling these models to effectively capture latent patterns. To address this challenge, we propose a novel framework, LLM-TPF, which leverages individuality and commonality fusion to enhance time series forecasting. In the frequency domain, periodic features are extracted to reveal the intrinsic periodicity of the data, while textual prototypes are used to indicate temporal trends. In the time domain, carefully designed prompts are employed to guide the models in comprehending global information. A commonality fusion mechanism further aggregates heterogeneous information across dimensions, and three distinct language models are utilized to independently process different types of information. Extensive real-world experiments demonstrate that LLM-TPF is a powerful tool for time series forecasting, achieving superior performance compared to state-of-the-art specialized models and exhibiting exceptional generalization ability in zero-shot scenarios. Code is available at https://github.com/switchsky/LLM-TPF.

1 Introduction

Time series forecasting holds a pivotal position in data science and machine learning as a critical technique for analyzing and predicting data patterns that evolve over time. It finds widespread applications across various domains, such as power system load prediction in energy sectors [Copiaco *et al.*, 2023], climate weather modeling [Huang *et al.*, 2023], and traffic flow analysis [Medina-Salgado *et al.*, 2022]. In recent years, pre-trained large language models (LLMs) have demonstrated remarkable potential across multiple fields, es-

*Xiangjie Kong is the corresponding author.

(a) Time Series Decomposition-Based Method
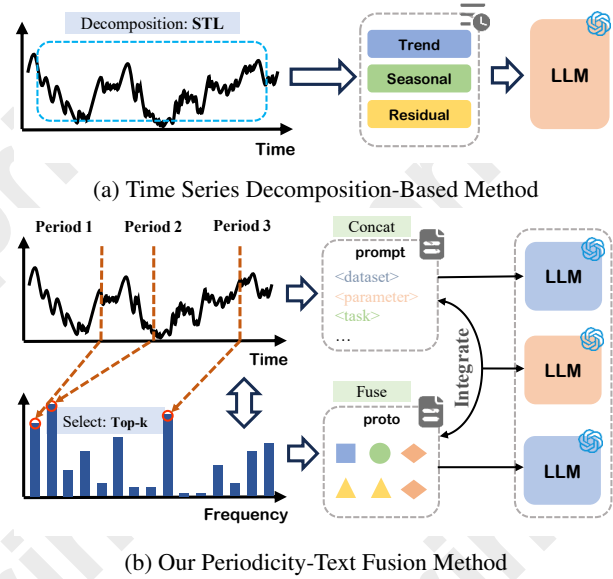

(b) Our Periodicity-Text Fusion Method

Figure 1: Difference between our approach and other integrations with LLMs. (a) Simply decomposing time series data leaves LLMs incapable of effectively understanding the periodic characteristics of the data. (b) Our approach, by integrating textual information (including prompts and textual prototypes) with time series information.

pecially excelling in few-shot and even zero-shot tasks [Zhao *et al.*, 2023].

Given that both time series and textual data share sequential characteristics, leveraging the strengths of LLMs in time series forecasting is a logical and promising direction. Numerous successful cases have already validated the efficacy of LLMs in this domain. For instance, [Tian Zhou, 2023] proposed a unified framework based on pre-trained language models, achieving significant performance improvements in various time series analysis tasks and laying a solid foundation for future research. TIME-LLM [Jin *et al.*, 2024] enriched the semantic representation of time series data through reprogramming, while CALF [Liu *et al.*, 2025] addressed the differences between text and time series data by processing these two modalities through separate branches, thus optimizing performance. Despite achieving impressive perfor-

mance in time series forecasting, the aforementioned methods still exhibit notable limitations. In particular, they fail to consider the periodic characteristics inherent in time series data (e.g., the Electricity dataset demonstrates clear seasonality and daily cycles). As shown in Figure 1, S^2IP-LLM [Pan *et al.*, 2024] and TEMPO [Cao *et al.*, 2024] incorporate trend decomposition to integrate time series data into large language models. However, since large language models are primarily trained on textual data, their ability to understand and model the periodic characteristics of time series remains limited.

To address these issues, we propose LLM-TPF, a pretrained LLM-based time series forecasting framework that explores how to extract temporal periodic information at different scales and bridge the gap between periodic features and the semantics of LLMs by integrating personalized and common feature fusion. To overcome the difficulty that LLMs face in interpreting periodic patterns in time series data, we propose the Personalized Frequency Domain Representation (PFD) module. This module extends time series data in the frequency domain and, by integrating refined textual prototypes, captures periodic features across different frequency ranges, thereby assisting the model in better grasping long-term trends and short-term fluctuations. Given the difficulty in capturing external information in time series, we further propose the Personalized Time Domain Representation (PTD) module, which uses carefully designed prompts to guide LLMs in perceiving and integrating external features, thereby generating time-domain representations with richer contextual semantics. Finally, to address potential redundancy or conflicts between frequency and time domain features, we design the Cross-Modal Common Feature Fusion (CMF) module, which efficiently integrates and extracts common representations from both feature types through a cross-modal attention mechanism. This fully leverages the advantages of multi-source features and significantly enhances the model's forecasting performance.

In summary, the contributions of our paper can be summarized as follows:

- We propose a novel framework named LLM-TPF that enhances semantic information by integrating the periodic characteristics of time series data. To the best of our knowledge, this is the first approach to address the integration of frequency and time domain understanding within large language models for time series analysis.

- The three proposed modules integrate temporal periodic information from the frequency domain and external information from the time domain. By freezing or fine-tuning the large language model, these modules effectively uncover latent features in time series data, enhancing its comprehension and modeling capabilities.

- Extensive experiments are conducted on seven real-world datasets, demonstrating that LLM-TPF achieves state-of-the-art performance in both long-term and short-term time series forecasting tasks. These results validate the effectiveness and practicality of our proposed method.

2 Related Work

2.1 Temporal Periodicity Analysis in Time Series

Latent features such as periodicity play a crucial role in improving the prediction accuracy of time series data. For instance, Autoformer [Wu *et al.*, 2021a] employs adaptive decomposition to separate trends and seasonal components, while FEDformer [Zhou *et al.*, 2022] enhances long-term forecasting using frequency-domain transformations. TimesNet [Wu *et al.*, 2023] further captures periodic features by transforming time series into a 2D frequency-domain representation, integrating multi-scale temporal and frequency information. The latest breakthrough, CycleNet [Lin *et al.*, 2024], explicitly models the periodic characteristics of data, achieving state-of-the-art performance across multiple domains using simple linear layers or shallow MLPs. Although numerous methods exist for extracting latent periodic features from time series data, such information remains challenging for large language models to comprehend effectively.

2.2 Time Series Forecasting Using LLMs

With the rise of LLMs, an increasing number of researchers have attempted to apply them to the field of time series forecasting. Tian Zhou and colleagues pioneered the integration of pretrained large models into time series prediction [Tian Zhou, 2023], designing adapter modules tailored for various downstream tasks, thereby enabling efficient transfer and application of LLMs in this domain. Following this, many researchers further explored prompt optimization strategies. For instance, TIME-LLM [Jin *et al.*, 2024] reformulates time series data into text-like representations more suitable for LLM processing, while CALF [Liu *et al.*, 2025] independently processes textual and time series data, employing sophisticated modules to bridge the gap between modalities.In contrast, models like S^2IP-LLM [Pan *et al.*, 2024] and TEMPO [Cao *et al.*, 2024] analyze latent periodic features within time series data and incorporate them into LLMs. However, current research has yet to fully exploit the periodic characteristics of time series data and lacks in-depth analysis across multiple scales.

2.3 Cross-modal Information Integration

Traditional multimodal fusion methods primarily focus on integrating data from different modalities. For instance, CLIP [Radford *et al.*, 2021] employs a dual-encoder to encode text and images separately, achieving cross-modal understanding via contrastive learning, while TCSP [Wu *et al.*, 2021b] enhances inter-modality interaction by optimizing modality fusion during feature extraction. In semantic segmentation, [Maiti *et al.*, 2023] introduces a framework tailored to specific scenarios, minimizing lossy preprocessing and boosting fusion efficiency. At the same time, UV-Mamba [Li *et al.*, 2024] utilizes deformable convolution networks to suppress state-space models and integrates multimodal features at the model level, fully leveraging the strengths of multiple models. Additionally, LLaVA [Liu *et al.*, 2023a] aligns segmented image data with prompt-based inputs and trains them using large language models. These studies provide valuable insights into exploring the integration of time-series data with large language models.

3 Methodology

3.1 Problem Definition

In traditional time series forecasting tasks, the dynamic features at time t can be represented as $X_t = (x_{t,1}, x_{t,2}, \cdots, x_{t,N})^\top \in \mathbb{R}^{N \times C}$, where $x_{t,c}$ is the feature vector of the c-th variable at time t, and C denotes the dimension of the feature variables. Additionally, we introduce a text prompt V to guide a large model in generating more precise time series forecasts. Specifically, $V \in \mathbb{R}^{L \times D}$ serves as the input prompt, where L represents the prompt length and D represents its dimensionality. Therefore, the time series forecasting problem can be simplified as follows: given the feature matrix of the past T_k time steps and the prompt information, predict the feature matrix for the next T_p time steps. This problem can be formalized as:

$$(X_{t-T_k+1:t}, V) \xrightarrow{f} X_{t+1:t+T_p}, \tag{1}$$

where $X_{t-T_k+1:t} \in \mathbb{R}^{T_k \times N \times C}$ represents the feature matrix of the past T_k time steps, $V \in \mathbb{R}^{L \times D}$ is the prompt matrix, and $X_{t+1:t+T_p} \in \mathbb{R}^{T_p \times N \times C}$ denotes the predicted feature matrix for the next T_p time steps.

3.2 Overall Architecture

Figure 2 shows the architecture of LLM-TPF, comprising three modules: the Personalized Representation of Frequency Domain (PFD), the Personalized Representation of Time Domain (PTD), and the Cross-Modal Common Feature Fusion (CMF). The PFD extracts periodic features, while the PTD generates personalized representations using prompt tokens [Jin *et al.*, 2024]. These features are fused by the CMF and decoded by a large language model, facilitating alignment and information sharing across modalities for better temporal and semantic modeling.

3.3 PFD Module

Frequency Domain Analysis

Traditional STL decomposition struggles with multi-scale and long-period time series. To address this, we use Fast Fourier Transform (FFT) to decompose the time series in the frequency domain, enabling effective analysis of different frequency components, as shown in Figure 3.

For a univariate time series $X_{pd} \in \mathbb{R}^{T \times C}$, its frequency domain representation is defined as:

$$A_j = \sum_{c=1}^{C} w_c \cdot |\text{FFT}(X_{pd,c})|_j, \tag{2}$$

where $\text{FFT}(\cdot)$ represents the Fast Fourier Transform, and A_j denotes the weighted absolute amplitude at frequency f_j, highlighting the significance of the periodic components. We apply a softmax function with a temperature parameter τ to convert amplitudes into a probability distribution, allowing us to prioritize the most significant frequencies. Specifically, the top-k frequencies $\{f_1, \ldots, f_k\}$ are selected based on the highest probabilities $P(f^*)$, where $f^* \in \{1, \ldots, \lfloor T/2 \rfloor\}$. The probability $P(f_j)$ is calculated as:

$$P(f_j) = \frac{\exp(A_j/\tau)}{\sum_{f^* \in \{1, \cdots, \lfloor T/2 \rfloor\}} \exp(A_{f^*}/\tau)}. \tag{3}$$

Due to the ability of 2D convolution to capture periodic characteristics at different scales [Wu *et al.*, 2023], effectively handling both long-term and short-term patterns, we adopt 2D convolution to reconstruct the time series into a 2D structure for aligning with periodic patterns and extracting temporal features:

$$\hat{X}_{2D}^i = \text{Reshape}_{p_i, f_i} \left(\text{Padding}(X_{pd}) \right), \tag{4}$$

$$\hat{X}_{pd}^i = \text{Reshape}_{1,(f_i \times p_i)} \left(\text{Conv2D} \left(\hat{X}_{2D}^i \right) \right). \tag{5}$$

Here, $\hat{X}_{2D}^i$ represents the padded and reshaped input with dimensions $p_i \times f_i$, where p_i and f_i are the selected period and frequency, respectively. The Conv2D operation extracts multi-scale periodic features, which are reshaped back into 1D as $\hat{X}_{pd}^i$.

Text Prototype Fusion

To address the challenge of accurately representing frequency-domain temporal information in large language models, we introduce PCA-based text prototype modeling method. By applying PCA to the vocabulary embedding matrix $A \in \mathbb{R}^{V \times D}$, we compress it into a lower-dimensional text prototype $E \in \mathbb{R}^{V' \times D}$:

$$E = \text{PCA}(A), \quad V' \ll V. \tag{6}$$

PCA focuses on retaining key components during dimensionality reduction, highlighting periodic and seasonal features while eliminating redundant noise. Subsequently, we fuse the temporal features $\hat{X}_{pd}^i$ with the text prototype E using a linear transformation and multi-head cross-attention mechanism to capture their deep associations:

$$Z_{\text{pd},i} = \text{softmax} \left(\frac{(W_X \hat{X}_{pd}^i + b_X)E^\top}{\sqrt{d_k}} \right) E,$$
$$Z_{\text{pd}} = \sum_{i=1}^{k} \alpha_i Z_{\text{pd},i}. \tag{7}$$

Here, W_X and b_X are learnable parameters, and Z_{pd} represents the aggregated periodic representation. The multi-head attention mechanism enables fine-grained fusion between temporal features and textual semantics, enriching the expression of periodic information. For example, when the time series data shows an upward trend over a specific period, it can be semantically represented as "growth" or "expansion" through text descriptions.

3.4 PTD Module

Prompts play a crucial role in generative AI models, serving as guides to steer the generation of desired outputs [Liu *et al.*, 2023b]. In the context of time-domain data, prompts can effectively assist large language models in capturing temporal information, thereby enhancing their prediction accuracy. To leverage this, we introduce time series data $X_{pd} \in \mathbb{R}^{T \times C}$, which is projected into the textual semantic space through a projection function $H(\cdot)$. The resulting representation is then
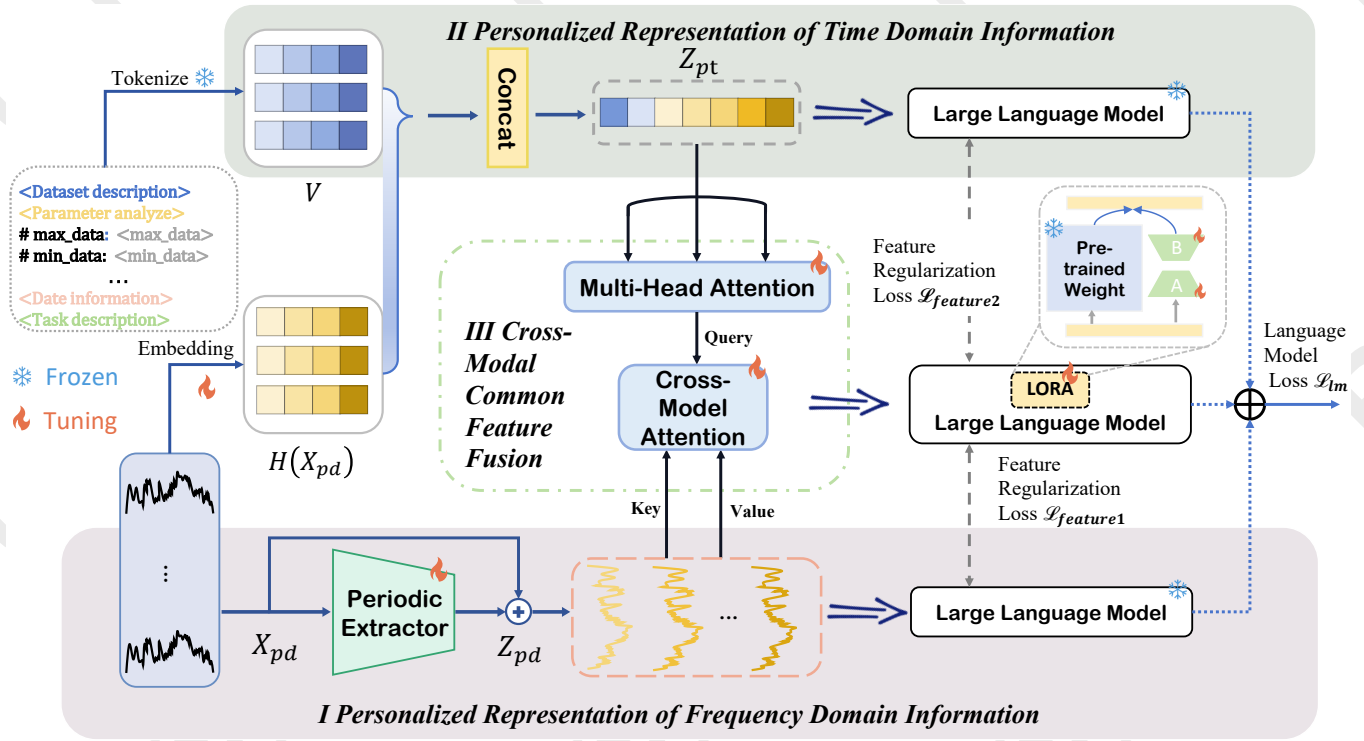
Figure 2: The overall framework of the proposed LLM-TPF: (I) Personalized Representation of Frequency Domain Information (PFD), which includes a Periodicity Extractor. (II) Personalized Representation of Time Domain Information (PTD). (III) a Cross-Modal Common Feature Fusion (CMF) module that integrates and interacts with the two personalized representations.
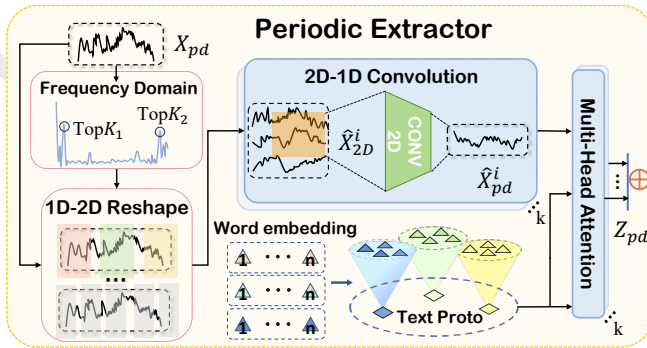

Figure 3: Internal Architectural Details of the Periodic Extractor.

concatenated with the prompt $V \in \mathbb{R}^{L \times P}$, creating a personalized prompt representation. This process is formalized as follows:

$$Z_{pt} = \text{Concat}(V, H(X_{pd})) \qquad (8)$$

Where $Z_{pt} \in \mathbb{R}^{(L+T) \times D}$ represents the concatenated personalized prompt representation, and $H(X_{pd}) \in \mathbb{R}^{T \times D}$ denotes the projected time series representation. Clear and precise prompts are essential for guiding large language models. We divide prompt construction into four components:

1. Summarizing the dataset in natural language;

2. Analyzing batch-specific parameters;

3. Incorporating temporal segmentation and date information;

4. Specifying task instructions.

Unlike [Jin *et al.*, 2024], which relies on batch statistics, our approach focuses on temporal segmentation and date factors, avoiding pattern traps [Satpute *et al.*, 2024]. This integration leverages the general knowledge of LLMs to infer deeper temporal insights, such as distinguishing between peak and off-peak electricity demand.

3.5 CMF Modules

Temporal information in the frequency and time domains represents two distinct modalities with significant differences. Drawing inspiration from the interactive fusion of individual and shared features across modalities, as explored in [Wu *et al.*, 2021b] for natural language and other modal data, we map these modalities into a unified feature space to learn a cohesive representation. Specifically, Z_{pt} is modeled using a multi-head self-attention mechanism to effectively capture interdependencies among the elements. The resulting fused representation, $\hat{Z}_{pt}$, is computed as follows:

$$\hat{Z}_{pt} = \text{MHSA}(Q, K, V) = \text{softmax}\left(\frac{QK^{\top}}{\sqrt{d_k}}\right)V, \qquad (9)$$
$$Q = W_Q Z_{pt}, \quad K = W_K Z_{pt}, \quad V = W_V Z_{pt}.$$

Here, W_Q, W_K, and W_V are linear projection matrices that map the concatenated features into the attention space. This

mechanism enhances cross-modal interactions and enables more accurate representation of temporal patterns. After obtaining the fused feature representation $\hat{Z}_{\text{pt}}$, redundant information may still persist. To refine cross-modal feature fusion, $\hat{Z}_{\text{pt}}$ is sparsified to remove redundancy before being processed alongside the frequency-domain representation $\hat{Z}_{\text{pd}}$ using the cross-modal attention mechanism (XMA). XMA compensates for missing periodicity and trends, producing a shared representation of the two modalities. The process is defined as:

$$\tilde{Z}_{\text{pt}} = \text{Dropout}(\hat{Z}_{\text{pt}}),$$
$$Z_{\text{sh}} = \text{XMA}(W_Q \tilde{Z}_{\text{pt}}, W_K \hat{Z}_{\text{pd}}, W_V \hat{Z}_{\text{pd}}). \quad (10)$$

Here, Z_{sh} represents the shared representation between the temporal data and the prompts, achieving efficient cross-modal feature integration by fusing critical information from different modalities.

3.6 Fine-Tuning Strategy and Loss Design

We have designed differentiated fine-tuning strategies for different LLMs to better accommodate the needs of personalized and generalized representations. For personalized representations, since personalized data often contains domain-specific details that do not require frequent updates, we choose to freeze the parameters of components handling personalized representations. This approach reduces computational overhead during training while preserving the model's original semantic understanding capabilities. For generalized representations, given their cross-domain nature and the need to adapt to diverse semantic environments, we employ Low-Rank Adaptation [Hu *et al.*, 2022] to achieve lightweight fine-tuning.

To ensure training stability and balance between personalized and generalized representations, we designed a three-branch guiding mechanism and introduced a feature regularization loss. The feature regularization loss is defined as:

$$\mathcal{L}_{\text{feature}} = \sum_{i=1}^{L} \gamma^{(L-i)} \sum_{b \in \{\text{pd,pt}\}} \text{sim}\big(\varphi_i^b(Y_b^i), \varphi_i^{\text{sh}}(Y_{\text{sh}}^i)\big), \quad (11)$$

The outputs Y_{pd}^i, Y_{pt}^i, and Y_{sh}^i represent the features from the i-th Transformer block for the PFD (pd), PTD (pt), and CMF (sh) modules. Here, $\varphi_i^b(\cdot)$ applies transformations to branch b, $\gamma^{(L-i)}$ assigns layer-specific weights, and $\text{sim}(\cdot, \cdot)$ measures feature similarity to encourage alignment. The total loss is defined as:

$$\mathcal{L}_{\text{total}} = \lambda_1 \mathcal{L}_{\text{feature}} + \lambda_2 \mathcal{L}_{\text{lm}}. \quad (12)$$

where $\mathcal{L}_{\text{feature}}$ is the feature alignment loss and $\mathcal{L}_{\text{lm}}$ represents the label alignment loss for multi-task learning. The weights λ_1 and λ_2 control the contribution of each loss term, with $\lambda_2 \gg \lambda_1$ to prioritize task label alignment.

4 Experiments

In this section, we comprehensively evaluate our model on various benchmark datasets covering long-term, short-term, and zero-shot forecasting tasks. We also analyze the model's design and present experimental results demonstrating its effectiveness and robustness across different scenarios.

4.1 Experimental Setup

Datasets. We will perform our experiments on eight diverse datasets from different domains with broad application contexts. For long-term forecasting, we utilize the ETT series with its four subsets (ETTh1, ETTh2, ETTm1, ETTm2), along with Weather, Traffic, and Electricity datasets, same as [Wu *et al.*, 2021a]. For short-term forecasting, we employ the M4 dataset, which includes marketing data spanning various years, quarters, and months.

Baseline. We conduct experiments with a selection of representative baseline models from recent years. These models can be categorized into four main types: (1) LLM-based methods: including Time-LLM [Jin *et al.*, 2024], OFA [Tian Zhou, 2023] and GPT-2 [Radford *et al.*, 2019]; (2) Transformer-based methods: including iTransformer [Liu *et al.*, 2024] and PatchTST [Nie *et al.*, 2023]; (3) CNN-based methods: including TimesNet [Wu *et al.*, 2023]; (4) Linear model-based methods: including DLinear [Zeng *et al.*, 2023].

Implementation Details. The experiments are performed on an NVIDIA RTX 3090 GPU with 24GB of memory. The Adam optimizer is employed to minimize the L1 loss, with the learning rate fixed at values within the set $\{1 \times 10^{-3}, 5 \times 10^{-4}, 1 \times 10^{-4}\}$. The large language model uses GPT-2 as the base model and employs LoRA for fine-tuning the large language model. A random seed of 2021 is used consistently throughout all experiments to ensure reproducibility.

4.2 Long-term and Short-term Forecasting

Long-term Forecasting

Table 1 highlights the significant superiority of LLM-TPF in long-term forecasting. As observed, our proposed model outperforms all baselines in most scenarios, particularly excelling on the ETT and Electricity datasets. TIME-LLM, a recent work, was the first to introduce the reprogramming of textual prototypes. Compared to TIME-LLM and TimesNet, we observed a 4% and 18% degradation in overall performance (measured by MAE) on the ETTh2 dataset, respectively. On the multivariate Electricity dataset, our model's performance dropped by 10% compared to another SOTA model, iTransformer. Nevertheless, these results underscore the notable advantages of our model in effectively handling multivariate and periodic data.

Short-term Forecasting

Our experimental results, which are presented in Table 2, demonstrate that our method outperforms other baselines on 80% of the evaluation metrics and achieves a 5.6% overall improvement compared to the state-of-the-art TIME-LLM. This advantage is likely due to our method's consideration of feature patterns across different time series scales.

4.3 Zero-shot Learning

Compared to traditional time series forecasting models, large language model-driven frameworks are expected to demonstrate zero-shot prediction capabilities. Specifically, a model optimized on a dataset X should exhibit strong predictive performance on an unseen target dataset Y, without requiring any prior exposure to samples from Y. As shown in Table 3,

Categories	LLM-based								Transformer-based				CNN-based		Linear-based	
Models	**LLM-TPF**		TIME-LLM		OFA		GPT-2		iTransformer		PatchTST		TimesNet		Dlinear	
Metrics	MSE	MAE	MSE	MAE	MSE	MAE	MSE	MAE	MSE	MAE	MSE	MAE	MSE	MAE	MSE	MAE
ETTh1 96	**0.368**	**0.386**	0.383	0.412	<u>0.379</u>	0.402	0.422	0.428	0.386	0.405	0.385	0.408	0.384	0.402	0.386	<u>0.400</u>
ETTh1 192	0.421	**0.418**	**0.408**	0.435	<u>0.415</u>	<u>0.424</u>	0.466	0.450	0.441	0.436	0.431	0.432	0.436	0.429	0.437	0.432
ETTh1 336	**0.425**	**0.429**	<u>0.426</u>	0.443	0.435	<u>0.440</u>	0.488	0.464	0.487	0.458	0.485	0.462	0.491	0.469	0.481	0.459
ETTh1 720	0.451	**0.455**	<u>0.443</u>	0.463	**0.441**	<u>0.459</u>	0.485	0.478	0.503	0.491	0.497	0.483	0.521	0.500	0.519	0.516
ETTh2 96	**0.271**	**0.326**	0.297	0.357	<u>0.289</u>	<u>0.347</u>	0.318	0.368	0.297	0.349	0.343	0.376	0.340	0.374	0.309	0.359
ETTh2 192	**0.343**	**0.373**	<u>0.349</u>	<u>0.390</u>	0.358	0.392	0.383	0.407	0.380	0.400	0.405	0.417	0.402	0.414	0.390	0.406
ETTh2 336	**0.350**	**0.387**	<u>0.373</u>	<u>0.408</u>	0.383	0.414	0.406	0.427	0.428	0.432	0.448	0.453	0.452	0.452	0.426	0.444
ETTh2 720	**0.398**	**0.422**	<u>0.400</u>	<u>0.436</u>	0.438	0.456	0.420	0.446	0.427	0.445	0.464	0.483	0.462	0.468	0.445	0.464
ETTm1 96	**0.283**	**0.343**	<u>0.291</u>	<u>0.346</u>	0.296	0.353	0.330	0.372	0.334	0.368	0.339	0.377	0.338	0.375	0.335	0.372
ETTm1 192	**0.321**	**0.372**	0.336	0.375	<u>0.335</u>	<u>0.373</u>	0.371	0.394	0.377	0.391	0.376	0.392	0.374	0.387	0.372	0.387
ETTm1 336	**0.353**	**0.381**	<u>0.362</u>	<u>0.390</u>	0.369	0.394	0.398	0.409	0.426	0.420	0.408	0.417	0.410	0.411	0.403	0.411
ETTm1 720	**0.405**	**0.417**	<u>0.410</u>	<u>0.421</u>	0.418	0.424	0.454	0.440	0.491	0.459	0.499	0.461	0.478	0.450	0.461	0.442
ETTm2 96	**0.173**	**0.251**	0.184	0.275	<u>0.174</u>	0.265	0.192	0.281	0.180	<u>0.264</u>	0.192	0.273	0.187	0.267	0.176	0.266
ETTm2 192	<u>0.235</u>	**0.295**	0.238	0.310	**0.231**	<u>0.306</u>	0.245	0.317	0.250	0.309	0.252	0.314	0.249	0.309	0.240	0.307
ETTm2 336	**0.275**	**0.334**	0.286	0.340	<u>0.280</u>	<u>0.339</u>	0.302	0.352	0.311	0.348	0.318	0.357	0.321	0.351	0.304	0.345
ETTm2 720	**0.361**	**0.387**	0.379	0.403	<u>0.373</u>	0.402	0.399	0.408	0.412	0.407	0.413	0.416	0.408	0.403	0.406	<u>0.400</u>
Weather 96	**0.153**	**0.207**	<u>0.158</u>	<u>0.210</u>	0.162	0.212	0.181	0.232	0.174	0.214	0.171	0.230	0.172	0.251	0.159	0.218
Weather 192	<u>0.201</u>	<u>0.247</u>	**0.197**	**0.245**	0.204	0.248	0.222	0.266	0.221	0.254	0.219	0.271	0.219	0.279	0.211	0.266
Weather 336	**0.243**	0.291	<u>0.248</u>	**0.285**	0.254	<u>0.286</u>	0.270	0.299	0.278	0.296	0.277	0.321	0.280	0.332	0.267	0.310
Weather 720	**0.318**	0.342	<u>0.319</u>	**0.334**	0.326	<u>0.337</u>	0.338	0.345	0.358	0.347	0.365	0.367	0.365	0.378	0.345	0.362
Electricity 96	**0.132**	0.238	<u>0.137</u>	0.244	0.139	**0.238**	0.138	0.234	0.148	0.240	0.159	0.268	0.168	0.288	0.159	0.268
Electricity 192	**0.149**	0.252	0.158	0.266	<u>0.153</u>	<u>0.251</u>	0.152	**0.247**	0.162	0.253	0.177	0.278	0.184	0.295	0.177	0.278
Electricity 336	**0.163**	**0.261**	0.183	0.292	<u>0.169</u>	0.266	0.168	<u>0.263</u>	0.178	0.269	0.195	0.296	0.198	0.312	0.195	0.296
Electricity 720	**0.200**	0.301	0.247	0.348	<u>0.206</u>	<u>0.297</u>	0.207	**0.295**	0.225	0.317	0.215	0.317	0.220	0.335	0.215	0.317
Traffic 96	**0.378**	<u>0.273</u>	<u>0.380</u>	0.277	0.388	0.282	0.390	**0.272**	0.395	0.268	0.583	0.319	0.593	0.329	0.570	0.310
Traffic 192	**0.392**	0.284	<u>0.399</u>	0.288	0.407	0.290	0.403	<u>0.277</u>	0.417	**0.276**	0.591	0.331	0.617	0.345	0.577	0.321
Traffic 336	0.413	**0.281**	**0.408**	0.290	<u>0.412</u>	0.294	0.447	0.298	0.433	<u>0.283</u>	0.599	0.332	0.629	0.339	0.588	0.324
Traffic 720	<u>0.447</u>	**0.293**	**0.445**	0.308	0.450	0.312	0.447	<u>0.298</u>	0.467	0.302	0.601	0.341	0.640	0.348	0.597	0.337

Table 1: Long-term forecasting results. We set the lookback window size T_k to 96 and the prediction length $T_p \in \{96, 192, 336, 720\}$. The best results are in **bold**, and the second-best are <u>underlined</u>.

Models		**LLM-TPF**	TIME-LLM	OFA	GPT-2	TimesNet	Dlinear
Yearly	SMAPE	**13.366**	<u>13.419</u>	13.531	15.11	15.378	16.965
	MASE	**2.99**	<u>3.005</u>	3.015	3.565	3.554	4.283
	OWA	**0.786**	<u>0.789</u>	0.793	0.911	0.918	1.058
Quarterly	SMAPE	<u>10.117</u>	**10.11**	10.177	10.597	10.465	12.145
	MASE	<u>1.179</u>	**1.178**	1.194	1.253	1.227	1.52
	OWA	**0.889**	<u>0.891</u>	0.898	0.938	0.936	1.106
Monthly	SMAPE	**12.854**	12.98	<u>12.894</u>	13.258	13.089	13.514
	MASE	**0.953**	0.963	<u>0.956</u>	1.003	0.996	1.037
	OWA	**0.895**	0.903	<u>0.897</u>	0.931	0.922	0.956
Others	SMAPE	**4.626**	<u>4.795</u>	4.94	6.124	6.599	6.709
	MASE	**3.116**	<u>3.178</u>	3.228	4.116	4.43	4.953
	OWA	**0.982**	<u>1.006</u>	1.029	1.259	1.393	1.487
Avg.	SMAPE	**11.915**	<u>11.983</u>	11.991	12.69	12.25	13.639
	MASE	**1.587**	<u>1.595</u>	1.6	1.808	1.698	2.095
	OWA	**0.854**	<u>0.859</u>	0.861	0.94	0.896	1.051

Table 2: Short-term Forecasting on the M4 Dataset. Prediction horizons range from [6, 48], with forecasting windows set to twice the lookback windows. Results are weighted averages across different sampling intervals.

Models	**LLM-TPF**		TIME-LLM		OFA		GPT-2	
Metrics	MSE	MAE	MSE	MAE	MSE	MAE	MSE	MAE
h1→ m1	**0.748**	**0.557**	0.847	0.565	<u>0.785</u>	<u>0.567</u>	0.798	0.574
h1→ m2	<u>0.314</u>	<u>0.354</u>	0.315	0.357	**0.305**	**0.347**	0.317	0.359
h2→ m1	**0.761**	**0.570**	<u>0.868</u>	<u>0.595</u>	0.877	0.601	0.920	0.610
h2→ m2	**0.311**	**0.354**	<u>0.322</u>	<u>0.363</u>	0.324	0.375	0.331	0.371

Table 3: Zero-shot learning results. The datasets "h1", "h2", "m1" and "m2" represent ETTh1, ETTh2, ETTm1 and ETTm2. All results are weighted averages across four different prediction lengths.

4.4 Model Analysis

Ablation Study

To validate the effectiveness of the proposed method, we conducted an ablation study on the ETTh2 and Electricity datasets, analyzing the model from four perspectives:

(1) **w/o PTD and PFD**: The personalized feature extraction modules are removed, and the raw temporal data are directly processed through self-attention before being passed to the large model.

(2) **w/o PFD**: The periodic features of the temporal data are omitted, leaving periodic information unextracted.

(3) **w/o CMF**: Cross-Modal Common Feature Fusion module is removed, and the model is restructured to a dual-channel processing framework.

(4) **w/o $\mathcal{L}_F$**: The weight of the regularization loss function is

we compare our proposed model with four baseline large language model-driven frameworks. Our model consistently outperforms the baselines in most scenarios. For instance, our approach achieves a reduction of 6.2% and 5.1% in error rates across all datasets compared to TIME-LLM and OFA, respectively. These results validate the effectiveness of our three-channel large language model design, which enables robust predictions without the need for task-specific training samples.

Components				Datasets	
PTD	PFD	CMF	$\mathcal{L}_F$	**ETTh2**	**Electricity**
	w/o or with			96 / 192 / 336	96 / 192 / 336
✗	✗	✓	✓	0.295 / 0.379 / 0.405	0.151 / 0.165 / 0.184
✓	✗	✓	✓	0.279 / 0.358 / 0.364	0.140 / 0.152 / 0.165
✓	✓	✗	✓	0.285 / 0.364 / 0.387	0.141 / 0.160 / 0.174
✓	✓	✓	✗	0.276 / 0.351 / 0.358	0.137 / 0.154 / 0.165
	LLM-TPF			**0.271 / 0.343 / 0.350**	**0.135 / 0.149 / 0.163**

Table 4: MSE Performance Evaluation on ETTh2 and Electricity Datasets with Ablation Analysis of Four Key Modules.

set to 0, effectively disabling the regularization constraint.

As shown in Table 4, the proposed LLM-TPF consistently outperforms all other ablation settings. In particular, the CMF module plays a critical role in the model's ability to effectively capture latent temporal features and guide the large language model. Furthermore, the appropriate use of regularization loss contributes to enhancing the model's stability, enabling it to perform robustly in complex temporal tasks.

The Effectiveness of the CMF Module

Figure 4 presents a comprehensive case analysis of the CMF module applied to the Electricity dataset for 96-step predictions. The top four subplots, labeled **(a)** through **(d)**, illustrate the optimization trajectory of the CMF module over different training epochs. The bottom section, represented by subplot **(e)**, provides an in-depth analysis of attention scores during epoch 13.

The left panel specifically explores the correlation between textual prompts and frequency-domain information, highlighting that textual features exhibit a stronger association with frequency-domain characteristics compared to time-domain data. By analyzing specific variables across various time steps and prompts, it becomes apparent that prompts enriched with external information, such as temporal context and dataset segmentation, are particularly effective in revealing latent temporal patterns, including periodicity, under certain conditions.

The right panel explores temporal representations within the time domain. Regions with high attention scores prominently exhibit periodic features, consistent with observations in the frequency domain, whereas regions with low attention scores lack discernible latent patterns. These findings highlight the complementary relationship between textual prompts, frequency-domain features, and temporal representations.

Hyperparameter Sensitivity

In this section, we investigate the impact of two key parameters in LLM-TPF on the overall performance of the model: 1) The Top-k parameter in the periodic layer of the PFD module, which determines the number of text prototypes introduced and the number of frequency domain layers considered during temporal feature analysis. 2) The regularization loss weight coefficient λ_1. In our experiments, we fixed $\lambda_2 = 1$ in the loss function and set the other two regularization loss weights to be equal for a more comparative analysis.

Figure 5 illustrates the overall performance of the model on the ETTh1 and Electricity datasets with respect to the two key parameters. It can be observed that when the top-k parameter
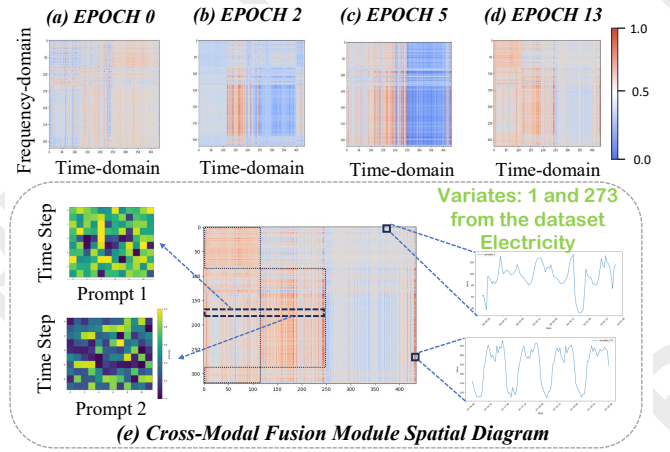

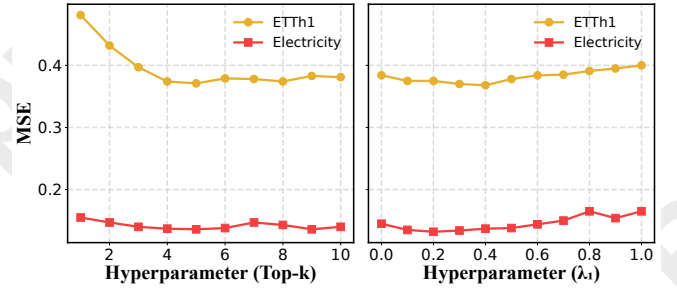Figure 4: Visualization of Cross-Attention Maps of the CMF Module for 96-Step Predictions on the Electricity Dataset.

Figure 5: Hyperparameter Study of Top-k Frequency Domain Layers and Regularization Loss Weight λ_1. (Prediction length: 96)

falls within the range of 4 to 6, the model achieves relatively better performance. This is because an appropriate number of textual prototypes facilitates the effective integration of latent temporal features. Conversely, a smaller top-k value may distort critical characteristics of the time series, such as periodicity or trends. The analysis further reveals that a moderate regularization loss weight coefficient λ_1 can effectively mitigate the learning bias of large language models. However, an excessively large λ_1 can prevent the model from correctly learning sample labels. In summary, hyperparameter design has limited impact, indicating the model's robustness to variations in top-k and λ_1.

5 Conclusion

In this paper, we propose LLM-TPF, a model with two personalized branches to capture latent features in time series data, including periodicity. Carefully designed prompts further guide the language model to generate more accurate time series predictions. Furthermore, we incorporate a shared branch to integrate temporal and frequency domain data, enabling LLMs to produce more accurate data representations. Experiments conducted on various datasets demonstrate the accuracy and effectiveness of our model. We hope that future research will further advance the application of LLM-TPF in larger-scale real-world scenarios.

Acknowledgments

References

[Cao *et al.*, 2024] Defu Cao, Furong Jia, Sercan O Arik, Tomas Pfister, Yixiang Zheng, Wen Ye, and Yan Liu. TEMPO: Prompt-based generative pre-trained transformer for time series forecasting. In *ICLR*, 2024.

[Copiaco *et al.*, 2023] Abigail Copiaco, Yassine Himeur, Abbes Amira, Wathiq Mansoor, Fodil Fadli, Shadi Atalla, and Shahab Saquib Sohail. An innovative deep anomaly detection of building energy consumption using energy time-series images. *Engineering Applications of Artificial Intelligence*, 119:105775, 2023.

[Hu *et al.*, 2022] Edward J Hu, Yelong Shen, Phillip Wallis, Zeyuan Allen-Zhu, Yuanzhi Li, Shean Wang, Lu Wang, and Weizhu Chen. LoRA: Low-rank adaptation of large language models. In *ICLR*, 2022.

[Huang *et al.*, 2023] Yiming Huang, Ziyu Zhou, Zihao Wang, Xiaoying Zhi, and Xiliang Liu. Timesnet-pm2. 5: Interpretable timesnet for disentangling intraperiod and interperiod variations in pm2. 5 prediction. *Atmosphere*, 14(11):1604, 2023.

[Jin *et al.*, 2024] Ming Jin, Shiyu Wang, Lintao Ma, Zhixuan Chu, James Y Zhang, Xiaoming Shi, Pin-Yu Chen, Yuxuan Liang, Yuan-Fang Li, Shirui Pan, and Qingsong Wen. Time-LLM: Time series forecasting by reprogramming large language models. In *ICLR*, 2024.

[Li *et al.*, 2024] Lulin Li, Ben Chen, Xuechao Zou, Junliang Xing, and Pin Tao. Uv-mamba: A dcn-enhanced state space model for urban village boundary identification in high-resolution remote sensing images. *arXiv preprint arXiv:2409.03431*, 2024.

[Lin *et al.*, 2024] Shengsheng Lin, Weiwei Lin, Xinyi Hu, Wentai Wu, Ruichao Mo, and Haocheng Zhong. Cyclenet: Enhancing time series forecasting through modeling periodic patterns. In *NeurIPS*, 2024.

[Liu *et al.*, 2023a] Haotian Liu, Chunyuan Li, Qingyang Wu, and Yong Jae Lee. Visual instruction tuning, 2023.

[Liu *et al.*, 2023b] Pengfei Liu, Weizhe Yuan, Jinlan Fu, Zhengbao Jiang, Hiroaki Hayashi, and Graham Neubig. Pre-train, prompt, and predict: A systematic survey of prompting methods in natural language processing. *CSUR*, 55(9):1–35, 2023.

[Liu *et al.*, 2024] Yong Liu, Tengge Hu, Haoran Zhang, Haixu Wu, Shiyu Wang, Lintao Ma, and Mingsheng Long. itransformer: Inverted transformers are effective for time series forecasting. In *ICLR*, 2024.

[Liu *et al.*, 2025] Peiyuan Liu, Hang Guo, Tao Dai, Naiqi Li, Jigang Bao, Xudong Ren, Yong Jiang, and Shu-Tao Xia. Calf: Aligning llms for time series forecasting via cross-modal fine-tuning. In *AAAI*, 2025.

[Maiti *et al.*, 2023] Abhisek Maiti, Sander Oude Elberink, and George Vosselman. Transfusion: Multi-modal fusion network for semantic segmentation. In *CVPR*, pages 6537–6547, 2023.

[Medina-Salgado *et al.*, 2022] Boris Medina-Salgado, Eddy Sánchez-DelaCruz, Pilar Pozos-Parra, and Javier E Sierra. Urban traffic flow prediction techniques: A review. *Sustainable Computing: Informatics and Systems*, 35:100739, 2022.

[Nie *et al.*, 2023] Yuqi Nie, Nam H. Nguyen, Phanwadee Sinthong, and Jayant Kalagnanam. A time series is worth 64 words: Long-term forecasting with transformers. In *ICLR*, 2023.

[Pan *et al.*, 2024] Zijie Pan, Yushan Jiang, Sahil Garg, Anderson Schneider, Yuriy Nevmyvaka, and Dongjin Song. S^2IP-LLM:semantic space informed prompt learning with llm for time series forecasting. In *ICML*, 2024.

[Radford *et al.*, 2019] Alec Radford, Jeff Wu, Rewon Child, David Luan, Dario Amodei, and Ilya Sutskever. Language models are unsupervised multitask learners. 2019.

[Radford *et al.*, 2021] Alec Radford, Jong Wook Kim, Chris Hallacy, Aditya Ramesh, Gabriel Goh, Sandhini Agarwal, Girish Sastry, Amanda Askell, Pamela Mishkin, Jack Clark, et al. Learning transferable visual models from natural language supervision. In *ICML*, pages 8748–8763, 2021.

[Satpute *et al.*, 2024] Ankit Satpute, Noah Gießing, André Greiner-Petter, Moritz Schubotz, Olaf Teschke, Akiko Aizawa, and Bela Gipp. Can llms master math? investigating large language models on math stack exchange. In *SIGIR*, pages 2316–2320, 2024.

[Tian Zhou, 2023] Xue Wang Liang Sun Rong Jin Tian Zhou, Peisong Niu. One Fits All: Power general time series analysis by pretrained lm. In *NeurIPS*, 2023.

[Wu *et al.*, 2021a] Haixu Wu, Jiehui Xu, Jianmin Wang, and Mingsheng Long. Autoformer: Decomposition transformers with auto-correlation for long-term series forecasting. In *NeurIPS*, volume 34, pages 22419–22430, 2021.

[Wu *et al.*, 2021b] Yang Wu, Zijie Lin, Yanyan Zhao, Bing Qin, and Li-Nan Zhu. A text-centered shared-private framework via cross-modal prediction for multimodal sentiment analysis. In *ACL*, pages 4730–4738, 2021.

[Wu *et al.*, 2023] Haixu Wu, Tengge Hu, Yong Liu, Hang Zhou, Jianmin Wang, and Mingsheng Long. Timesnet: Temporal 2d-variation modeling for general time series analysis. In *ICLR*, 2023.

[Zeng *et al.*, 2023] Ailing Zeng, Muxi Chen, Lei Zhang, and Qiang Xu. Are transformers effective for time series forecasting? In *AAAI*, volume 37, pages 11121–11128, 2023.

[Zhao *et al.*, 2023] Wayne Xin Zhao, Kun Zhou, Junyi Li, Tianyi Tang, Xiaolei Wang, Yupeng Hou, Yingqian Min, Beichen Zhang, Junjie Zhang, Zican Dong, et al. A survey of large language models. *arXiv preprint arXiv:2303.18223*, 2023.

[Zhou *et al.*, 2022] Tian Zhou, Ziqing Ma, Qingsong Wen, Xue Wang, Liang Sun, and Rong Jin. Fedformer: Frequency enhanced decomposed transformer for long-term series forecasting. In *ICML*, pages 27268–27286, 2022.